HHS Public Access

Author manuscript

Radiat Res. Author manuscript; available in PMC 2015 September 01.

Published in final edited form as:

Radiat Res. 2015 August ; 184(2): 121–133.

Global Metabolomic Identification of Long-Term Dose-Dependent Urinary Biomarkers in Nonhuman Primates Exposed to Ionizing Radiation

Evan L. Pannkuk[a], **Evagelia C. Laiakis**[a], **Simon Authier**[b], **Karen Wong**[b], and **Albert J. Fornace Jr.**[a,c,d,1]

[a]Department of Biochemistry and Molecular & Cellular Biology, Georgetown University Medical Center, Washington, DC

[b]CiToxLAB North America, Laval, Canada

[c]Lombardi Comprehensive Cancer Center, Georgetown University, Washington, DC

[d]Center of Excellence in Genomic Medicine Research, King Abdulaziz University, Jeddah 22254, Saudi Arabia

Abstract

Due to concerns surrounding potential large-scale radiological events, there is a need to determine robust radiation signatures for the rapid identification of exposed individuals, which can then be used to guide the development of compact field deployable instruments to assess individual dose. Metabolomics provides a technology to process easily accessible biofluids and determine rigorous quantitative radiation biomarkers with mass spectrometry (MS) platforms. While multiple studies have utilized murine models to determine radiation biomarkers, limited studies have profiled nonhuman primate (NHP) metabolic radiation signatures. In addition, these studies have concentrated on short-term biomarkers (i.e., <72 h). The current study addresses the need for biomarkers beyond 72 h using a NHP model. Urine samples were collected at 7 days postirradiation (2, 4, 6, 7 and 10 Gy) and processed with ultra-performance liquid chromatography (UPLC) quadrupole time-of-flight (QTOF) MS, acquiring global metabolomic radiation signatures. Multivariate data analysis revealed clear separation between control and irradiated groups. Thirteen biomarkers exhibiting a dose response were validated with tandem MS. There was significantly higher excretion of L-carnitine, L-acetylcarnitine, xanthine and xanthosine in males versus females. Metabolites validated in this study suggest perturbation of several pathways including fatty acid β oxidation, tryptophan metabolism, purine catabolism, taurine metabolism and steroid hormone biosynthesis. In this novel study we detected long-term biomarkers in a NHP model after exposure to radiation and demonstrate differences between sexes using UPLC-QTOF-MS-based metabolomics technology.

[1]Address for correspondence: Georgetown University, 3970 Reservoir Road, NW, New Research Building, Room E504, Washington, DC 20057; af294@georgetown.edu.

INTRODUCTION

Due to increased terrorist threats and the most recent nuclear accident at the Fukushima Nuclear Power Plant, there has been an increasing awareness of, and need for, medical countermeasures to potential radiological and nuclear exposures (1, 2). One such need is the development of clinical and field-based diagnostic tools for biodosimetry and the determination of individual radiation exposure. Such biodosimetry tools will aid assessment of potentially irradiated individual's need for critical care and treatment classification that will facilitate both immediate and long-term treatment (3). With the ensuing, mounting panic and public unrest after a radiological event, the development and availability of compact biodosimetry tools capable of utilizing noninvasive biofluids would also aid in minimizing public distress. Metabolomics (analysis of molecules <1 kDa) technology is a relatively new approach for the rapid high-throughput analysis of easily accessible biofluids, such as urine or blood, to assess individual radiation exposure (4, 5). Furthermore, multiple studies have utilized ultra-performance liquid chromatography (UPLC) quadrupole time-of-flight (QTOF) mass spectrometry (MS) platforms to show consistent inducible biomarkers from ionizing radiation (6–11). Because metabolic profiling with MS platforms has now become a potentially powerful and innovative biodosimetry tool, there is a need to identify metabolomics based time-dependent radiation signatures.

Development of field-based biodosimetry devices requires appropriate animal models for testing radiation injury and identification of radiation biomarkers (12, 13). Studies measuring radiation-induced metabolic changes have included mice (10, 11, 14–16), rats (6, 9, 17–19), nonhuman primates (NHPs) (7, 20) and humans undergoing total-body irradiation (TBI) (8). NHP models are advantageous due to the closer genetic similarity to humans over other animal models (i.e., murine models), the ability to minimize exogenous variability (e.g., diet) and intraspecific genetic differences seen in human studies (8). In addition, a wealth of information has been collected on primary radiation exposure effects in NHP models, such as postirradiation hematopoiesis (21, 22), damage to the gastrointestinal (GI) tract (23–25) and kidney (26). The acute and prolonged GI syndromes have been described and categorized in detail in total- and partial-body-irradiated NHPs (23, 24). While NHP responses to radiation exposure have been well characterized, metabolomic data on NHP tissues and biofluids is lacking, since only a limited number of studies have analyzed NHP samples using high-throughput global metabolomics (7, 20). In one study, 13 metabolites were identified by UPLC-QTOF-MS and were determined to significantly increase after 8.5 Gy irradiation, with the highest increases at 24 h (except tyrosol sulfate) (7). The identified biomarkers suggested perturbations to fatty acid β-oxidation pathways, lowered muscle conversion of creatine and oxidative damage to DNA. In another study, a targeted approach was applied to quantitate citrulline levels in serum from irradiated NHPs (20). Citrulline has been proposed as a biomarker of acute GI syndrome after radiation exposure. While these studies provide valuable baseline information and validated biomarker quantification methodology, more knowledge is needed on long-term biomarkers to aid human triage.

The current study directly addresses the need for long-term biomarkers (i.e., >72 h) to aid in triage after radiation exposure. In the event of a radiological or nuclear incident, establishment of field sites for biofluid processing could occur within hours or days.

However, individuals may be unable to reach such sites for extended time periods. As metabolic biodosimetry is challenged by time-dependent responses, and can be complicated by individual differences and preexisting medical conditions, adequate knowledge of short- and long-term metabolic perturbations due to radiation exposure is required (27). The purpose of the current study is to add to existing known radiation biomarkers, thus aiding the development of field- and clinical-based biodosimetry tools. We determined 7-day biomarkers in NHP urine after gamma irradiation (2, 4, 6, 7 and 10 Gy) utilizing global metabolic profiling with UPLC-QTOF-MS. In addition to investigating the dose response of specific biomarkers, sex differences were assessed for the generation of male- or female-specific signatures, as previously determined in humans (8). In addition to unique biomarkers, we found increased excretion of metabolites indicative of specific metabolic perturbations that overlap with studies in other species. Importantly, identified biomarkers exhibited dose-dependent concentration changes. To the best of our knowledge, this is the first published study to determine biomarkers in a NHP model at 7 days after radiation exposure and to document differences between sexes using UPLC-QTOF-MS-based metabolomics.

MATERIALS AND METHODS

Chemicals

All reagents were LC-MS grade (Fisher Scientific Inc., Hanover Park, IL) and chemicals (debrisoquine sulfate, 4-nitrobenzoic acid, xanthosine, kynurenic acid, L-carnitine, hypoxanthine, cortisol, cortisone, creatine, creatinine, xanthine, taurine, L-acetylcarnitine, xanthurenic acid (all Sigma-Aldrich® LLC, St. Louis, MO) and isobutyryl-L-carnitine (Santa Cruz Biotechnology® Inc., Dallas, TX) were the highest purity available.

Nonhuman Primate System and Experimental Treatments

A total of 108 adult rhesus macaque animals (*Macaca mulatta*; 54 males, 54 females, 3.6–5.9 years old and weighing ~ 4.65 kg) of Chinese origin, were acclimated to environmental conditions for at least 6 weeks prior to study initiation. Purified water was provided *ad libitum* to all animals and food consumption evaluated at least twice daily. Animals received a certified chow twice daily (Teklad Certified Hi-Fiber Primate Diet no. 7195C; Harlan® Laboratories, Madison, WI). Animals were monitored continuously (i.e., 24 h/day) by veterinarians for any clinical signs of distress or pain and the experimental protocol included strict euthanasia criteria reviewed and approved by the Institutional Animal Care and Use Committee. No animal presented clinical signs that warranted euthanasia per these pre-established criteria.

Animals were positioned in a symmetrical position prior to a single TBI at a dose rate of ~0.6 Gy/min with a ^{60}Co gamma source on day 0. Animals received ondansetron (2.0 mg/ml, 1.5 mg/kg) preirradiation as antiemetic and lactated Ringer's solution (5.0 ml/kg) postirradiation for hydration. Starting on day 3, animals received buprenorphine (0.01–0.02 mg/kg) at least twice daily as preemptive analgesia. Six male and six female animals were assigned to a control group or treatment group receiving 2, 4, 6, 7 or 10 Gy TBI. These doses were administered to span sublethal, hematopoietic and minor gastrointestinal

syndromes. TBI dose was determined with two dosimeters (scanned nanoDots™, Landauer®, Glenwood, IL) placed on each animal during irradiation (one midplane of xiphoid process and one interscapular region) and a Farmer® ionization chamber (model no. TN30013; PTW, Freiburg, Germany) connected to an electrometer (model no. 34050; Keithley Instruments Inc., Cleveland, Ohio). Clinical examinations, body weight/dimensions and clinical pathology (i.e., hematology) were performed on all animals preirradiation and seven days postirradiation.

Urine Collection

Urine was collected from control and irradiated groups on day 7 and stored at −70°C until shipment on dry ice to Georgetown University Medical Center. Urine (≤1.0 ml) was collected with a syringe by cystocentesis for treatment groups. Urine from the control group was collected overnight, with food and water removed prior to urine collection. Urine was collected from 6 males and 6 females exposed to all radiation levels except for the following groups: female, 2 Gy ($n = 4$); female, 10 Gy ($n = 4$); and male, 4 Gy ($n = 5$).

Sample Preparation and Analysis

Samples were prepared and analyzed as previously described (8). Briefly, urine (50.0 μl) was mixed with 50.0 μl acetonitrile (ACN; 1:1 dilution) and internal standards [4.0 μ*M* debrisoquine $(M + H)^+ = 176.1188$; 30.0 μ*M* 4-nitrobenzoic acid $(M - H)^- = 166.0141$], incubated on ice for 10 min and centrifuged for 15 min (maximum speed, 4°C).

Samples were injected (5.0 μl) into an UPLC coupled to a Premier® QTOF-MS (Waters® Corp., Milford, MA) equipped with a Waters ACQUITY® BEH C18 1.7 μm, 2.1 × 100 mm column in both negative and positive electrospray ionization (ESI) modes as previously described (8). Sulfamethoxine [$(M + H)^+ = 311.0814$; $(M - H)^- = 309.0685$)] was used for the Lock-Spray® mass reference.

Data Processing, Statistical Analysis and Marker Validation

The total ion chromatogram (TIC) was deconvoluted and peak aligned using the MarkerLynx™XS Application Manager (Waters Corp.). Preprocessed data from control and irradiated groups was analyzed with the in-house statistical package MetaboLyzer (17) for univariate analysis and the machine learning algorithm Random Forests (RF) through the programing language R. Ions present ≥70% (complete-presence ions) across samples were identified, log transformed, normalized to a Gaussian curve and analyzed with a Welch's *t* test ($P < 0.05$). Ions present ≤70% (partial-presence ions) across samples were treated as categorical data and analyzed with discrete statistics [i.e., Fisher's exact test ($P < 0.05$)]. Complete presence data were further analyzed with an unsupervised principal component analysis (PCA; with unit scaling, linear singular value decomposition, 3 maximum decision-tree depth) using an in-house software and Python programing language. Nontransformed complete presence data were compared with RF decision-tree learning (9). A multidimensional scaling plot and heatmap were constructed from all metabolites in positive and negative mode. Putative statistically significant ions were identified through the human metabolome database (HMDB) or the database and ontology of chemical entities of biological interest (ChEBI) (28, 29). GraphPad Prism 6 software was used to graph validated

ions and compare hematology results with an unpaired *t* test with equal standard deviation (La Jolla, CA). Putatively identified ions were validated by UPLC-QTOF tandem MS. Pure standards were diluted in 1:1 ACN:H_2O and fragmented with a 5–50 eV ramped collision energy. Fragmentation patterns and retention times were compared to putative metabolites in NHP urine and cross-referenced with the METLIN tandem MS database (30).

RESULTS

Clinical Pathology

Animals that were 7 and 10 Gy irradiation exhibited signs of decreased physical activity and decreased appetite with an associated ~6.8% (7 Gy) and ~14.0% (10 Gy) decrease in body weight. Hematology results (compared with an unpaired *t* test with equal standard deviation) significantly declined in males and females in all exposed groups, except platelet count (Supplementary Table S1; http://dx.doi.org/10.1667/RR14091.1.S1). Lymphocyte counts confirmed the high radiosensitivity of this lineage with a dose-dependent decrease after irradiation. The platelet count significantly increased at 2 Gy, was not significantly different at 4 and 6 Gy and significantly decreased at 7 and 10 Gy. These hematologic changes are expected after radiation exposure (31).

Biomarker Identification and Validation

Ions from deconvoluted (MarkerLynx™XS), transformed (MetaboLyzer), and normalized (MetaboLyzer) datasets were compared between controls and differing radiation levels with a Welch's *t* test (presence >70%). Creatinine significantly decreased and was therefore not suitable for data normalization. Detection of ions that reached statistical significance ($P < 0.05$) were putatively identified at 2 Gy (296 ESI^+, 311 ESI^-), 4 Gy (352 ESI^+, 294 ESI^-), 6 Gy (427 ESI^+, 416 ESI^-), 7 Gy (392 ESI^+, 337 ESI^-) and 10 Gy (414 ESI^+, 288 ESI^-) compared to the control data set. Ions with a presence <70% were analyzed as categorical data with a Fischer's exact test. Partial presence significant ions ($P < 0.05$), were putatively identified at 2 Gy (140 ESI^+, 196 ESI^-), 4 Gy (201 ESI^+, 167 ESI^-), 6 Gy (256 ESI^+, 268 ESI^-), 7 Gy (203 ESI^+, 203 ESI^-) and 10 Gy (489 ESI^+, 643 ESI^-) compared to the control data set.

Databases comparing putative ions by univariate statistics between control and irradiated NHPs were mined and 25 ions of interest were selected for validation by tandem MS. Thirteen ions were validated (Figs. 1–2; Table 1). Isobutyryl-L-carnitine and its isomer, butyrylcarnitine, could not be differentiated due to identical mass and similar fragmentation pattern. Of the 13 validated ions, significant increased excretion (represented as: detected adduct, radiation dose eliciting first significant difference, fold change at specified radiation dose) of isobutyryl-L-carnitine/butyrylcarnitine [$(M + H)^+$, 2 Gy, 1.1-fold), L-carnitine ($M + H)^+$, 4 Gy, 14.6-fold), L-acetylcarnitine [$(M + H)^+$, 4 Gy, 8.6-fold), taurine [$(M - H)^-$, 2 Gy, 2.2-fold), xanthurenic acid [$(M - H)^-$, 2 Gy, 2.0-fold), cortisol [$(M + H)^+$, 2 Gy, 2.1-fold), cortisone [$(M + H)^+$, 2 Gy, 1.6-fold) and kynurenic acid [$(M + H)^+$, 6 Gy, 1.3-fold] was observed. Two deaminated products of guanine and adenine, hypoxanthine [$(M + H)^+$, 2 Gy, 1.7-fold and xanthosine $(M - H)^-$, 2 Gy, 2.2-fold], previously identified in urine after irradiation were detected in the current study (7, 8, 11). Hypoxanthine and xanthosine were

significantly excreted at higher levels at 2 Gy, stayed constant at 4, 6 and 7 Gy and further increased at 10 Gy. Another deaminated purine (xanthine) increased at 2 Gy ($P = 0.2$) and 10 Gy ($P = 0.6$), but not significantly. Significantly lower excretion of xanthine was observed at 4 Gy ($P = 0.03$) and 6 Gy ($P = 0.04$). Creatine significantly decreased at 2 Gy [$(M + H)^+$, 2 Gy, 0.2-fold] but increased at higher doses (e.g., 7.7-fold increase at 10 Gy). Creatinine [$(M + H)^+$, 6 Gy, 0.5-fold] significantly decreased. Twelve biomarkers were significantly different at 10 Gy (Table 2). The remaining biomarkers were not validated and are listed as putative (Supplementary Table S2; http://dx.doi.org/10.1667/RR14091.1.S1). Eight acylcarnitines and nine acylglycines were also putatively identified (Supplementary Table S3; http://dx.doi.org/10.1667/RR14091.1.S1).

Multivariate Data Analysis

Unsupervised PCA models were developed for control urine samples compared to 2, 4, 6, 7 and 10 Gy day 7 postirradiation datasets (Fig. 3). Clear separation among control and irradiated samples occurs at 6, 7 and 10 Gy exposure levels, a pattern that has been previously reported at earlier time points after irradiation (7). The datasets were also analyzed with the machine-learning algorithm RF. A total of 2,392 ions from the ESI^+ dataset gave an accuracy of 56.1% (60.6% for top 100 metabolites) and 3,004 ions from the ESI^- dataset gave an accuracy of 51.5% (56.1% for top 100 metabolites). A multidimensional scaling plot shows separation among the control and all treatment groups in positive and negative modes. In agreement with the PCA models, 2 and 4 Gy irradiations overlap with increasing separation at 6, 7 and 10 Gy (Fig. 4). Differences among control and irradiated groups are also shown as a heatmap of the top 50 ions (Fig. 4B). Five validated metabolites [creatine (19), L-acetylcarnitine (73), cortisol (84), L-carnitine (61), isobutyryl-L-carnitine/butyrylcarnitine (89)] were identified in the top 100 metabolites by RF analysis.

Differences between Males and Females

We chose to concentrate on sex differences at 7 Gy due to unequal sample sizes at 10 Gy exposure. A PCA plot indicates control groups cluster together, suggesting few differences between males and females not exposed to radiation (Fig. 5A). There are more pronounced differences in the 7 Gy irradiated group (Fig. 5B). Significant complete presence (155 ESI^+, 156 ESI^-) and partial presence (8 ESI^+, 8 ESI^-) ions were putatively identified. Of the previously validated biomarkers, L-carnitine ($P = 0.02$), L-acetylcarnitine ($P = 0.01$), xanthine ($P < 0.001$) and xanthosine ($P < 0.001$) were significantly higher in males than females (Fig. 6). L-carnitine may be an inherent sex difference, as it was significantly higher in the female control group than the male control ($P = 0.02$). While L-carnitine and L-acetylcarnitine excretion significantly increased in both sexes after radiation exposure, the fold change was greater in males than in females (L-carnitine = 3.99 and 3.03, respectively; L-acetylcarnitine = 10.76 and 3.48, respectively). Xanthosine increased in females at 7 Gy, but not significantly from the control group. Xanthine did not significantly change between the control and 7 Gy irradiated group, however, females exhibited a decrease in xanthine concentration while males exhibited an increased excretion (Fig. 6).

DISCUSSION

In this study, we performed untargeted metabolomics to determine urinary biomarkers in NHPs 7 days after exposure to radiation. We validated 13 possible biomarkers and putatively identified another 24 compounds for assessing 7-day postirradiation injury (Table 1). These metabolites suggest perturbation of several pathways including fatty acid β oxidation, tryptophan metabolism, purine catabolism, taurine metabolism and steroid hormone biosynthesis. Sex differences were observed, specifically, excretion levels of L-carnitine, L-acetylcarnitine, xanthine and xanthosine were significantly higher in males than in females. These sex differences may suggest an enhanced radiation effect on fatty acid β oxidation, purine catabolism and ultimately increased oxidative stress in male NHPs. The determination of radiation-induced metabolites from global profiling experiments will allow for the development of targeted approaches aiding in diagnostics and instrument technologies. With improved biodosimetry from metabolomics technology and development of field-deployable instrumentation, one could accurately and quickly determine large-scale injury after a radiological event. Subsequently, these studies may aid in the national effort for an improved strategic plan after a nuclear or radiological event.

Previous metabolomic profiling studies on NHP urine over a 3-day time course postirradiation identified altered levels of 13 metabolites that may serve as possible biomarkers of radiation injury (Table 3) (7). Xanthine (8.5 Gy), hypoxanthine (3.5 Gy) and uric acid (6.5 Gy) levels were elevated, indicating DNA damage. Compounds involved in taurine metabolism (i.e., taurine, *N*-acetyltaurine and isethionic acid) were elevated after exposure to 6.5 and 8.5 Gy of radiation. Creatine and creatinine both increased after 6.5 Gy irradiation, indicating renal damage and lowered muscle conversion of creatine. Other biomarkers included tyramine sulfate, *N*-acetylserotonin sulfate, 3-hydroxytyrosol sulfate, tyrosol sulfate and adipic acid (7). In humans, hypoxanthine, uric acid, xanthine, L-octanoylcarnitine, N6,N6,N6-trimethyl-L-lysine, acetyl-DL-carnitine and decanoylcarnitine were determined as urinary biomarkers of radiation exposure (8). Consistent with NHP models, uric acid and xanthine were excreted in higher levels in irradiated humans indicating increased oxidative stress.

We found increased levels of xanthine, hypoxanthine and xanthosine, which are involved in purine catabolism and either likely excreted after damage to DNA from ionizing radiation exposure or are products of increased oxidative stress. The nitrogenous base material comprising RNA and DNA include specific purines (adenine and guanine) and pyrimidines (uracil, thymine and cytosine). Hypoxanthine is formed from inosine (EC:3.2.2.2; EC: 3.2.2.1; EC:3.2.2.8) or is a deaminated product of adenine (EC:3.5.4.2). Xanthine can be a deaminated product of guanine (EC:3.5.4.3), converted either from hypoxanthine (EC: 1.17.1.4, EC:1.17.3.2) or from xanthosine (EC:3.2.2.1). These metabolites are commonly observed in global metabolomics studies of ionizing radiation and have been discussed in detail elsewhere (7, 8, 11, 32).

Three carnitine metabolites (L-carnitine, isobutyryl-L-carnitine/butyrylcarnitine and L-acetylcarnitine) involved in mitochondrial fatty acid β oxidation were elevated in NHP urine after radiation exposure. Fatty acid β oxidation is responsible for generating ketone bodies

for energy production when glucose levels are low (33). Carnitine, acetylcarnitine and long-chain acylcarnitines play key roles in fatty acid β oxidation by facilitating free fatty acid (FFA) transport into the mitochondrial matrix (Fig. 7). Fatty acid transport proteins (FATPs) actively uptake FFAs into cells (34). Long-chain acyl-CoA ligase (ACSL) binds nonpolar hydrophobic FFAs to CoA and produces water-soluble acyl-CoAs. Unable to pass the inner mitochondrial membrane, acyl-CoA is bound to L-carnitine by carnitine palmitoyl-transferase I (CPTI; EC:2.3.1.21), producing esterified acylcarnitines (Supplementary Fig. S1; http://dx.doi.org/10.1667/RR14091.1.S1). Carnitine acylcarnitine translocase (CACT; GeneID: 788; integral to mitochondrial inner membrane) transports the long-chain acylcarnitine into the mitochondrial matrix, subsequently converting to acyl-CoA ester by CPTII. Acyl-CoA is subsequently catabolized to acetyl-CoAs through β oxidation, ultimately entering the tricarboxylic acid cycle (TCA cycle) and electron-transport chain for energy production.

Carnitine (and several of their acyl-ester) biomarkers have been identified from other species exposed to different radiation sources (Supplementary Fig. S1; http://dx.doi.org/10.1667/RR14091.1.S1). As previously mentioned, acetyl-DL-carnitine, L-octanoylcarnitine, decanoylcarnitine and N6,N6,N6-trimethyl-L-lysine (TML, an endogenous carnitine precursor) were identified as urinary biomarkers in humans exposed to 1.25 Gy TBI (Supplementary Fig. S2; http://dx.doi.org/10.1667/RR14091.1.S1) (8). The overall decreased excretion of TML, L-octanoylcarnitine and acetyl-DL-carnitine suggests increased intracellular β oxidation. In mouse models, O-propanoylcarnitine was elevated in urine after an intraperitoneal stressor injection (lipopolysaccharide) and 3, 8 and 15 Gy gamma-radiation exposure (15). Tiglylcarnitine, hexanoylcarnitine and propanoylcarnitine decreased in mouse urine exposed to 1.1 Gy low-dose-rate (0.00309 Gy/min) X irradiation but increased when radiation was delivered at a high-dose rate (1.03 Gy/min) (35). Tiglylcarnitine and hexanoylcarnitine excretion decreased in mouse urine exposed to internal 1.95 Gy ^{137}Cs after 48 h (mimicking effects observed with low-dose-rate irradiation) (36). Clearly, inflammatory conditions, dose and dose rate and internal or external exposure can affect the interpretation of carnitine conjugates as radiation biomarkers. Perturbations to carnitine regulation are implicated in myriad diseases and conditions, including liver disorders (37), obesity (37), trauma (38) and malnutrition (39, 40), among others (reviewed in 41).

Kynurenic acid and xanthurenic acid are tryptophan metabolic products and possible biomarkers of renal failure (42), vitamin B6 deficiency, tuberculosis, exposure to radiation (14, 35, 36) and can induce mitochondrial damage (43). Tryptophan is metabolized primarily through the kynurenine pathway with a small percentage metabolized through the serotonin pathway. Tryptophan is oxidized to form formylkynurenine, which is hydrolyzed to kynurenine (Supplementary Fig. S3; http://dx.doi.org/10.1667/RR14091.1.S1). Kynurenine aminotransferases (KATs) convert kynurenine to kynurenic acid. Kynurenine may also be hydroxylated by kynurenine 3-hydroxylase to form 3-hydroxykynurenine. KATs also convert toxic 3-hydroxykynurenine to xanthurenic acid for excretion. Interestingly, while these metabolite concentrations increased and are indicative of renal failure, the concentration of creatinine decreased in a dose-dependent manner. Increased serum/urine creatinine levels are a well-known biomarker of renal failure (44, 45). Creatine

is synthesized or obtained through diet in vertebrates, transported in blood and actively transported to tissues such as muscles for energy production. Creatine is degraded into creatinine, which is then excreted in the urine by active transport (~10–40%) and passive filtration in the glomerulus (46). Reduced creatinine production has been observed in patients with muscle wasting, malnutrition and lower body mass index (47). As body weight was reduced up to 14%, this phenomenon may explain the discrepancy with past observed dose responses.

Cholesterol metabolism is important in steroids/hormone synthesis and may be affected after radiation exposure. Plasma cholesterol and triacylglyceride levels were perturbed in individuals exposed to radiation from the Chernobyl incident (48). Numerous other studies for determining low-dose ^{137}Cs ingestion in rats showed minor molecular modifications of hepatic cholesterol metabolism with few physiological symptoms or homeostasis perturbations after chronic ingestion for a period of 3 (49), 9 (50) and 10 months (51). In the current study, two cholesterol-derived glucocorticoids, cortisol (2 Gy, 2.1-fold) and cortisone (2 Gy, 1.6-fold) were found in higher concentration in samples from irradiated animals. Previously, rats exposed to ^{137}Cs in drinking water for 9 months exhibited decreased 17β-estradiol levels (threefold), increased corticosterone levels (1.3-fold), but unaffected aldosterone levels (52). Biologically inactive cortisone is reduced to active cortisol mineralocorticoid by 11β-hydroxysteroid dehydrogenase type 1 (EC:1.1.1.146). As increased cortisol levels may also contribute to stress (53) and hypertension (54), glucocorticoids and neurotransmitters may be indicative of general stress after the radiological event rather than a direct product from exposure to radiation.

Sex differences were observed as shown in a previous human study (8). Xanthine, xanthosine, L-carnitine and L-acetylcarnitine were excreted in significantly higher levels in males vs. females. While L-carnitine was observed to be higher in control females compared to males, the fold change was reported to be greater in male humans exposed to 1.25 Gy TBI (8). These results may indicate increased perturbations to fatty acid β oxidation and purine catabolism in males, however, the precise mechanism is unclear. Estrogen has been shown to protect against damage from radiation exposure (55), which may play a role in dose response observed in this study. The identification of sex-specific factors responsible for differences in response to radiation exposure remains to be elucidated.

Of concern to national security is public exposure (accidental and intentional) to radiation. Currently, field-and clinical-based biodosimetry tools for rapid assessment of radiation injury from easily accessible biofluids are limited in nature. Metabolomics offers a technology for rapid assessment of an individual’s health and detection of possible perturbations from exposure to radiation. Development of biodosimetry tools requires proper animal models to bridge with murine studies and ultimately predict human responses. NHP models are advantageous to murine models due to increased genetic similarities with humans (hence similar phenotypic responses during the prodromal syndrome (e.g., vomiting and diarrhea), which are the target group for field-based biodosimetry tools. With only a single study reporting on the identification of radiation biomarkers in NHP urine, metabolomic studies on radiation-induced damage in NHP models are lacking. Furthermore, previous studies have identified biomarkers at short post-exposure time frames (e.g., 24–72

h), while individuals seeking medical help for exposure after a radiological event may be unable to immediately reach hospitals or rescue units. At a 7-day time point other identified radiation biomarkers may have leveled out to preirradiation levels. Here we provide long-term radiation-induced biomarkers in NHP urine and contribute to the current state of a "radiation biomarker library". Future studies should include effects of age, partial-body irradiation and pre-existing conditions on metabolomic radiation signatures. These results will aid in the development of biodosimetry tools for radiation injury assessment, effective triage and appropriate medical intervention.

Supplementary Material

Refer to Web version on PubMed Central for supplementary material.

Acknowledgments

This work was funded by the National Institutes of Health (National Institute of Allergy and Infectious Diseases grant no. 1R01AI101798; P.I. Albert J. Fornace, Jr.). The authors acknowledge and thank the Lombardi Comprehensive Cancer Proteomics and Metabolomics Shared Resource for data acquisition, which is partially supported by the National Cancer Institute (award no. P30CA051008; P.I. Louis Weiner). The authors also thank John Moulder, Brian Fish, Eric Cohen and Eric Weh of the Medical College of Wisconsin for advice on kidney function. The content of this article is solely the responsibility of the authors and does not necessarily represent the official views of the National Cancer Institute or the National Institutes of Health.

References

1. Dicarlo AL, Ramakrishnan N, Hatchett RJ. Radiation combined injury: overview of NIAID research. Health Phys. 2010; 98:863–7. [PubMed: 20445395]
2. Dicarlo AL, Jackson IL, Shah JR, Czarniecki CW, Maidment BW, Williams JP. Development and licensure of medical countermeasures to treat lung damage resulting from a radiological or nuclear incident. Radiat Res. 2012; 177:717–21. [PubMed: 22468704]
3. Swartz HM, Flood AB, Williams BB, Meineke V, Dorr H. Comparison of the needs for biodosimetry for large-scale radiation events for military versus civilian populations. Health Phys. 2014; 106:755–63. [PubMed: 24776910]
4. Coy SL, Krylov EV, Schneider BB, Covey TR, Brenner DJ, Tyburski JB, et al. Detection of radiation-exposure biomarkers by differential mobility prefiltered mass spectrometry (DMS-MS). Int J Mass Spectrom. 2010; 291:108–17. [PubMed: 20305793]
5. Coy SL, Cheema AK, Tyburski JB, Laiakis EC, Collins SP, Fornace AJ. Radiation metabolomics and its potential in biodosimetry. Int J Radiat Biol. 2011; 87:802–23. [PubMed: 21692691]
6. Johnson CH, Patterson AD, Krausz KW, Lanz C, Kang DW, Luecke H, et al. Radiation metabolomics. 4. UPLC-ESI-QTOFMS-based metabolomics for urinary biomarker discovery in gamma-irradiated rats. Radiat Res. 2011; 175:473–84. [PubMed: 21309707]
7. Johnson CH, Patterson AD, Krausz KW, Kalinich JF, Tyburski JB, Kang DW, et al. Radiation metabolomics. 5. Identification of urinary biomarkers of ionizing radiation exposure in nonhuman primates by mass spectrometry-based metabolomics. Radiat Res. 2012; 178:328–40. [PubMed: 22954391]
8. Laiakis EC, Mak TD, Anizan S, Amundson SA, Barker CA, Wolden SL, et al. Development of a metabolomic radiation signature in urine from patients undergoing total body irradiation. Radiat Res. 2014; 181:350–61. [PubMed: 24673254]
9. Lanz C, Patterson AD, Slavik J, Krausz KW, Ledermann M, Gonzalez FJ, et al. Radiation metabolomics. 3. Biomarker discovery in the urine of gamma-irradiated rats using a simplified metabolomics protocol of gas chromatography-mass spectrometry combined with random forests machine learning algorithm. Radiat Res. 2009; 172:198–212. [PubMed: 19630524]

10. Tyburski JB, Patterson AD, Krausz KW, Slavik J, Fornace AJ Jr, Gonzalez FJ, et al. Radiation metabolomics. 1. Identification of minimally invasive urine biomarkers for gamma-radiation exposure in mice. Radiat Res. 2008; 170:1–14. [PubMed: 18582157]
11. Tyburski JB, Patterson AD, Krausz KW, Slavik J, Fornace AJ Jr, Gonzalez FJ, et al. Radiation metabolomics. 2. Dose- and time-dependent urinary excretion of deaminated purines and pyrimidines after sublethal gamma-radiation exposure in mice. Radiat Res. 2009; 172:42–57. [PubMed: 19580506]
12. Augustine AD, Gondre-Lewis T, Mcbride W, Miller L, Pellmar TC, Rockwell S. Animal models for radiation injury, protection and therapy. Radiat Res. 2005; 164:100–9. [PubMed: 15966769]
13. Williams JP, Brown SL, Georges GE, Hauer-Jensen M, Hill RP, Huser AK, et al. Animal models for medical countermeasures to radiation exposure. Radiat Res. 2010; 173:557–78. [PubMed: 20334528]
14. O Broin P, Vaitheesvaran B, Saha S, Hartil K, Chen EI, Goldman D, et al. Intestinal microbiota-derived metabolomic blood plasma markers for prior radiation injury. Int J Radiat Oncol Biol Phys. 2015; 91:360–7. [PubMed: 25636760]
15. Laiakis EC, Hyduke DR, Fornace AJ. Comparison of mouse urinary metabolic profiles after exposure to the inflammatory stressors gamma radiation and lipopolysaccharide. Radiat Res. 2012; 177:187–99. [PubMed: 22128784]
16. Khan AR, Rana P, Devi MM, Chaturvedi S, Javed S, Tripathi RP, et al. Nuclear magnetic resonance spectroscopy-based metabonomic investigation of biochemical effects in serum of gamma-irradiated mice. Int J Radiat Biol. 2011; 87:91–7. [PubMed: 21087167]
17. Mak TD, Tyburski JB, Krausz KW, Kalinich JF, Gonzalez FJ, Fornace AJ Jr. Exposure to ionizing radiation reveals global dose-and time-dependent changes in the urinary metabolome of rat. Metabolomics. 2014:1–13.10.1007/s11306-014-0765-4
18. Tang X, Zheng M, Zhang Y, Fan S, Wang C. Estimation value of plasma amino acid target analysis to the acute radiation injury early triage in the rat model. Metabolomics. 2013; 9:853–63.
19. Zhang Y, Zhou X, Li C, Wu J, Kuo JE, Wang C. Assessment of early triage for acute radiation injury in rat model based on urinary amino acid target analysis. Mol Biosyst. 2014; 10:1441–9. [PubMed: 24647718]
20. Jones JW, Tudor G, Bennett A, Farese AM, Moroni M, Booth C, et al. Development and validation of a LC-MS/MS assay for quantitation of plasma citrulline for application to animal models of the acute radiation syndrome across multiple species. Anal Bioanal Chem. 2014; 406:4663–75. [PubMed: 24842404]
21. Bogden AE, Eltringham JR, Anderson DR. Effect of total body irradiation on the immune response of rhesus monkeys to a single antigenic stimulus. Radiat Res. 1970; 42:90–104. [PubMed: 4985520]
22. Gengozian N, Moriarty C, Good RA. Functional evaluation of T helper, T suppressor, and B lymphocytes in lethally irradiated rhesus monkeys injected with autologous bone marrow. Transplantation. 1992; 53:1313–22. [PubMed: 1534940]
23. Macvittie TJ, Farese AM, Bennett A, Gelfond D, Shea-Donohue T, Tudor G, et al. The acute gastrointestinal subsyndrome of the acute radiation syndrome: a rhesus macaque model. Health Phys. 2012; 103:411–26. [PubMed: 22929470]
24. Macvittie TJ, Bennett A, Booth C, Garofalo M, Tudor G, Ward A, et al. The prolonged gastrointestinal syndrome in rhesus macaques: the relationship between gastrointestinal, hematopoietic, and delayed multi-organ sequelae following acute, potentially lethal, partial-body irradiation. Health Phys. 2012; 103:427–53. [PubMed: 22929471]
25. Vigneulle RM, Rao S, Fasano A, Macvittie TJ. Structural and functional alterations of the gastrointestinal tract following radiation-induced injury in the rhesus monkey. Dig Dis Sci. 2002; 47:1480–91. [PubMed: 12141804]
26. Van Kleef EM, Zurcher C, Oussoren YG, Te Poele JA, Van Der Valk MA, Niemer-Tucker MM, et al. Long-term effects of total-body irradiation on the kidney of Rhesus monkeys. Int J Radiat Biol. 2000; 76:641–8. [PubMed: 10866286]

27. Swartz HM, Flood AB, Gougelet RM, Rea ME, Nicolalde RJ, Williams BB. A critical assessment of biodosimetry methods for large-scale incidents. Health Phys. 2010; 98:95–108. [PubMed: 20065671]
28. Wishart DS, Knox C, Guo AC, Eisner R, Young N, Gautam B, et al. HMDB: a knowledgebase for the human metabolome. Nucleic Acids Res. 2009; 37:D603–10. [PubMed: 18953024]
29. Degtyarenko K, De Matos P, Ennis M, Hastings J, Zbinden M, Mcnaught A, et al. ChEBI: a database and ontology for chemical entities of biological interest. Nucleic Acids Res. 2008; 36:D344–50. [PubMed: 17932057]
30. Zhu ZJ, Schultz AW, Wang J, Johnson CH, Yannone SM, Patti GJ, et al. Liquid chromatography quadrupole time-of-flight mass spectrometry characterization of metabolites guided by the METLIN database. Nat Protoc. 2013; 8:451–60. [PubMed: 23391889]
31. Dainiak N. Hematologic consequences of exposure to ionizing radiation. Exp Hematol. 2002; 30:513–28. [PubMed: 12063018]
32. Manna SK, Krausz KW, Bonzo JA, Idle JR, Gonzalez FJ. Metabolomics reveals aging-associated attenuation of noninvasive radiation biomarkers in mice: Potential role of polyamine catabolism and incoherent DNA damage-repair. J Proteome Res. 2013; 12:2269–81. [PubMed: 23586774]
33. Rinaldo P, Matern D, Bennett MJ. Fatty acid oxidation disorders. Annu Rev Physiol. 2002; 64:477–502. [PubMed: 11826276]
34. Houten SM, Wanders RJ. A general introduction to the biochemistry of mitochondrial fatty acid beta-oxidation. J Inherit Metab Dis. 2010; 33:469–77. [PubMed: 20195903]
35. Goudarzi M, Mak TD, Chen C, Smilenov LB, Brenner DJ, Fornace AJ. The effect of low dose rate on metabolomic response to radiation in mice. Radiat Environ Biophys. 2014; 53:645–57. [PubMed: 25047638]
36. Goudarzi M, Weber W, Mak TD, Chung J, Doyle-Eisele M, Melo D, et al. Development of urinary biomarkers for internal exposure by cesium-137 using a metabolomics approach in mice. Radiat Res. 2014; 181:54–64. [PubMed: 24377719]
37. Cave MC, Hurt RT, Frazier TH, Matheson PJ, Garrison RN, Mcclain CJ, et al. Obesity, inflammation, and the potential application of pharmaconutrition. Nutr Clin Pract. 2008; 23:16–34. [PubMed: 18203961]
38. Biolo G, Toigo G, Ciocchi B, Situlin R, Iscra F, Gullo A, et al. Metabolic response to injury and sepsis: changes in protein metabolism. Nutrition. 1997; 13:52S–7S. [PubMed: 9290110]
39. Khan L, Bamji MS. Plasma carnitine levels in children with protein-calorie malnutrition before and after rehabilitation. Clin Chim Acta. 1977; 75:163–6. [PubMed: 403033]
40. Khan L, Bamji MS. Tissue carnitine deficiency due to dietary lysine deficiency: triglyceride accumulation and concomitant impairment in fatty acid oxidation. J Nutr. 1979; 109:24–31. [PubMed: 430211]
41. Flanagan JL, Simmons PA, Vehige J, Willcox MD, Garrett Q. Role of carnitine in disease. Nutr Metab (Lond). 2010; 7:30. [PubMed: 20398344]
42. Pawlak D, Tankiewicz A, Mysliwiec P, Buczko W. Tryptophan metabolism via the kynurenine pathway in experimental chronic renal failure. Nephron. 2002; 90:328–35. [PubMed: 11867954]
43. Malina HZ, Richter C, Mehl M, Hess OM. Pathological apoptosis by xanthurenic acid, a tryptophan metabolite: activation of cell caspases but not cytoskeleton breakdown. BMC Physiol. 2001; 1:7. [PubMed: 11459518]
44. Levey AS, Perrone RD, Madias NE. Serum creatinine and renal function. Annu Rev Med. 1988; 39:465–90. [PubMed: 3285786]
45. Wyss M, Kaddurah-Daouk R. Creatine and creatinine metabolism. Physiol Rev. 2000; 80:1107–213. [PubMed: 10893433]
46. Lepist EI, Zhang X, Hao J, Huang J, Kosaka A, Birkus G, et al. Contribution of the organic anion transporter OAT2 to the renal active tubular secretion of creatinine and mechanism for serum creatinine elevations caused by cobicistat. Kidney Int. 2014; 86:350–7. [PubMed: 24646860]
47. Beddhu S, Samore MH, Roberts MS, Stoddard GJ, Pappas LM, Cheung AK. Creatinine production, nutrition, and glomerular filtration rate estimation. J Am Soc Nephrol. 2003; 14:1000–5. [PubMed: 12660334]

48. Chaialo PP, Chobot'ko GM, Shimelis IV, Prevarskii BP. Content of blood lipids and characteristics of dyslipoproteinemias in people exposed to radiation during the accident at the Chernobyl nuclear power station. Ukr Biokhim Zh. 1991; 63:93–6. [PubMed: 1816692]

49. Souidi M, Tissandie E, Grandcolas L, Grison S, Paquet F, Voisin P, et al. Chronic contamination with 137cesium in rat: effect on liver cholesterol metabolism. Int J Toxicol. 2006; 25:493–7. [PubMed: 17132608]

50. Racine R, Grandcolas L, Grison S, Gourmelon P, Gueguen Y, Veyssiere G, et al. Molecular modifications of cholesterol metabolism in the liver and the brain after chronic contamination with cesium 137. Food Chem Toxicol. 2009; 47:1642–7. [PubMed: 19394396]

51. Racine R, Grandcolas L, Blanchardon E, Gourmelon P, Veyssierre G, Souidi M. Hepatic cholesterol metabolism following a chronic ingestion of cesium-137 starting at fetal stage in rats. J Radiat Res. 2010; 51:37–45. [PubMed: 20173315]

52. Grignard E, Gueguen Y, Grison S, Lobaccaro JM, Gourmelon P, Souidi M. In vivo effects of chronic contamination with 137 cesium on testicular and adrenal steroidogenesis. Arch Toxicol. 2008; 82:583–9. [PubMed: 18046538]

53. De Kloet ER, Joels M, Holsboer F. Stress and the brain: from adaptation to disease. Nat Rev Neurosci. 2005; 6:463–75. [PubMed: 15891777]

54. Whitworth JA, Williamson PM, Mangos G, Kelly JJ. Cardiovascular consequences of cortisol excess. Vasc Health Risk Manag. 2005; 1:291–9. [PubMed: 17315601]

55. Dynlacht JR, Valluri S, Lopez J, Greer F, Desrosiers C, Caperell-Grant A, et al. Estrogen protects against radiation-induced cataractogenesis. Radiat Res. 2008; 170:758–64. [PubMed: 19138041]

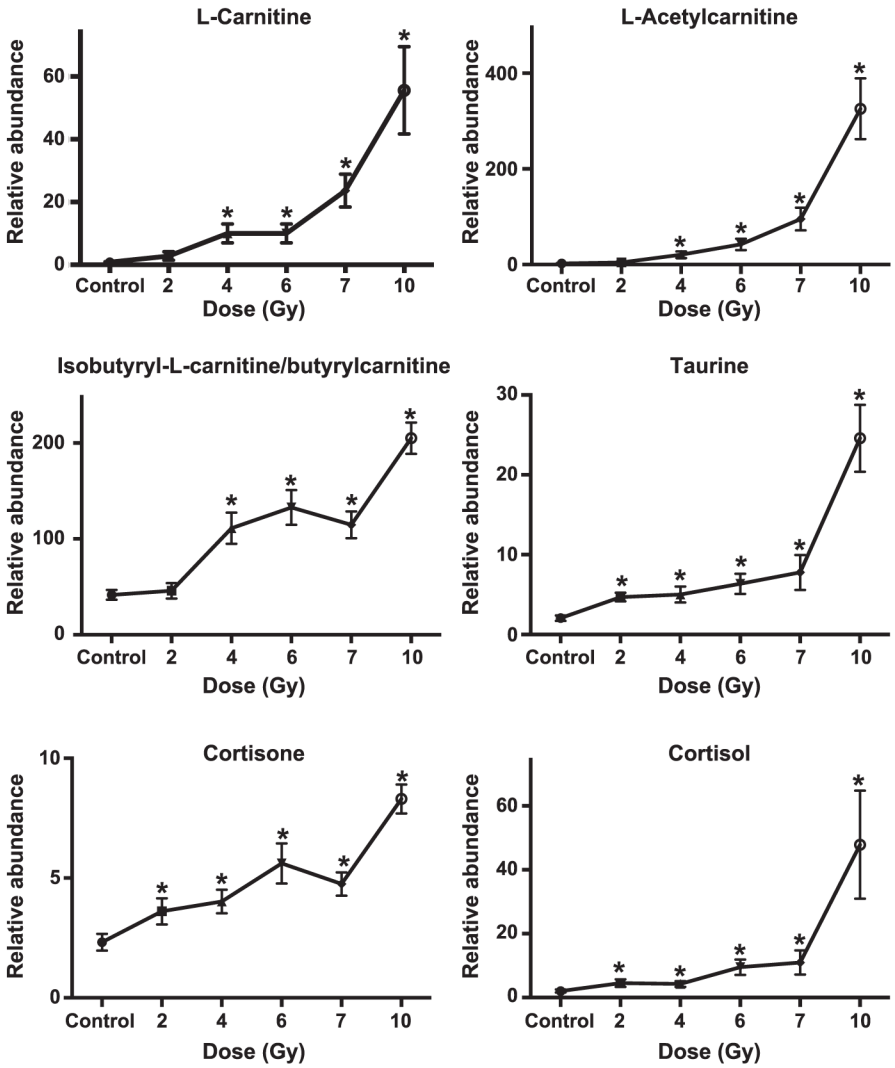

FIG. 1.

Dose response of urinary biomarkers (carnitine, acylcarnitines, sterols and taurine) in nonhuman primates (NHPs) exposed to 2, 4, 6, 7 and 10 Gy gamma radiation (mean ± SEM). Dose response was compared to the control using Welch's *t* test [*significantly different from control ($P < 0.05$)]. Significant increases in taurine, isobutyryl-L-carnitine/butyrylcarnitine and sterols were observed at all doses compared to the control. L-carnitine and L-acetylcarnitine were significantly excreted at 4 Gy and higher.

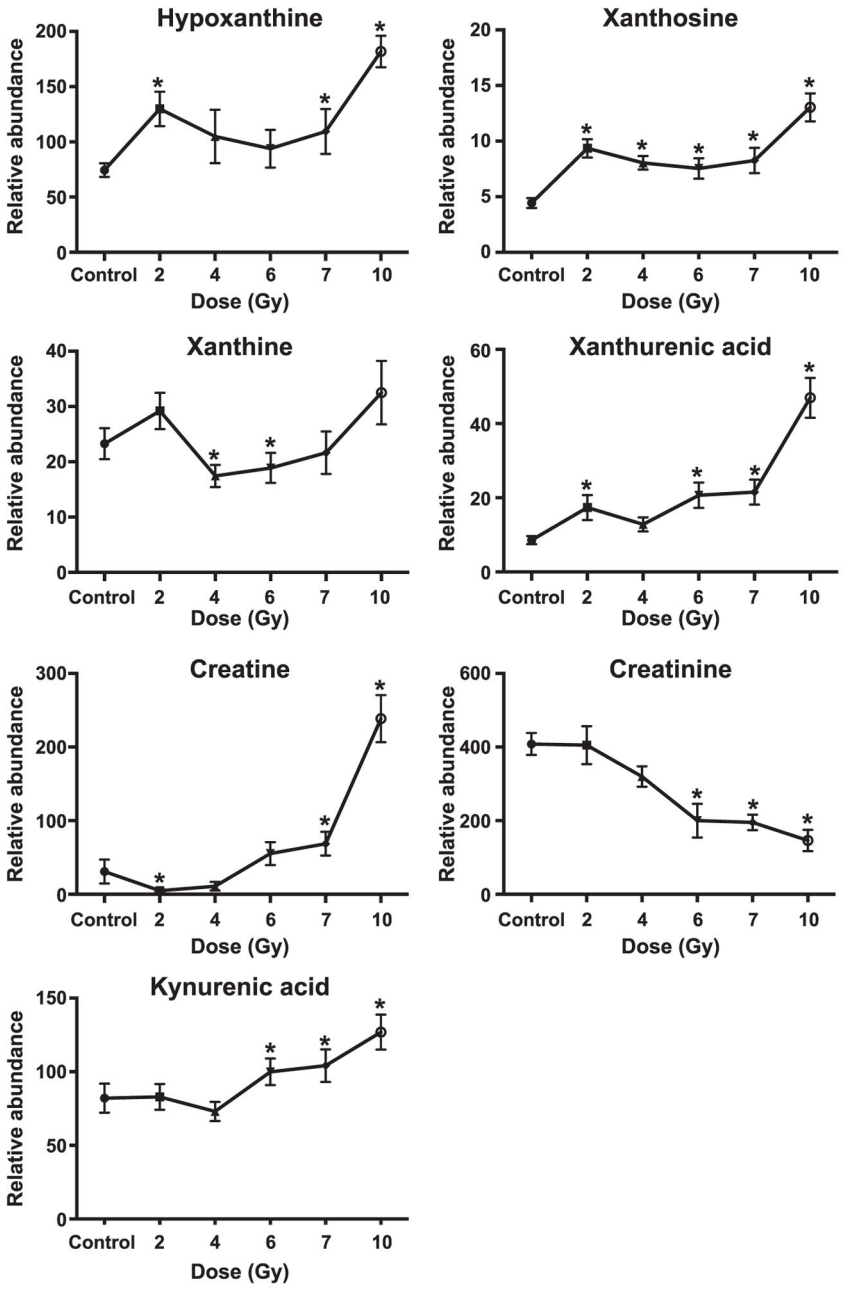

FIG. 2.

Dose response of urinary biomarkers from NHPs exposed to 2, 4, 6, 7 and 10 Gy gamma radiation [mean ± SEM; *significantly different from control ($P < 0.05$)]. Increased excretion of xanthurenic acid and kynurenic acid suggests impaired renal function.

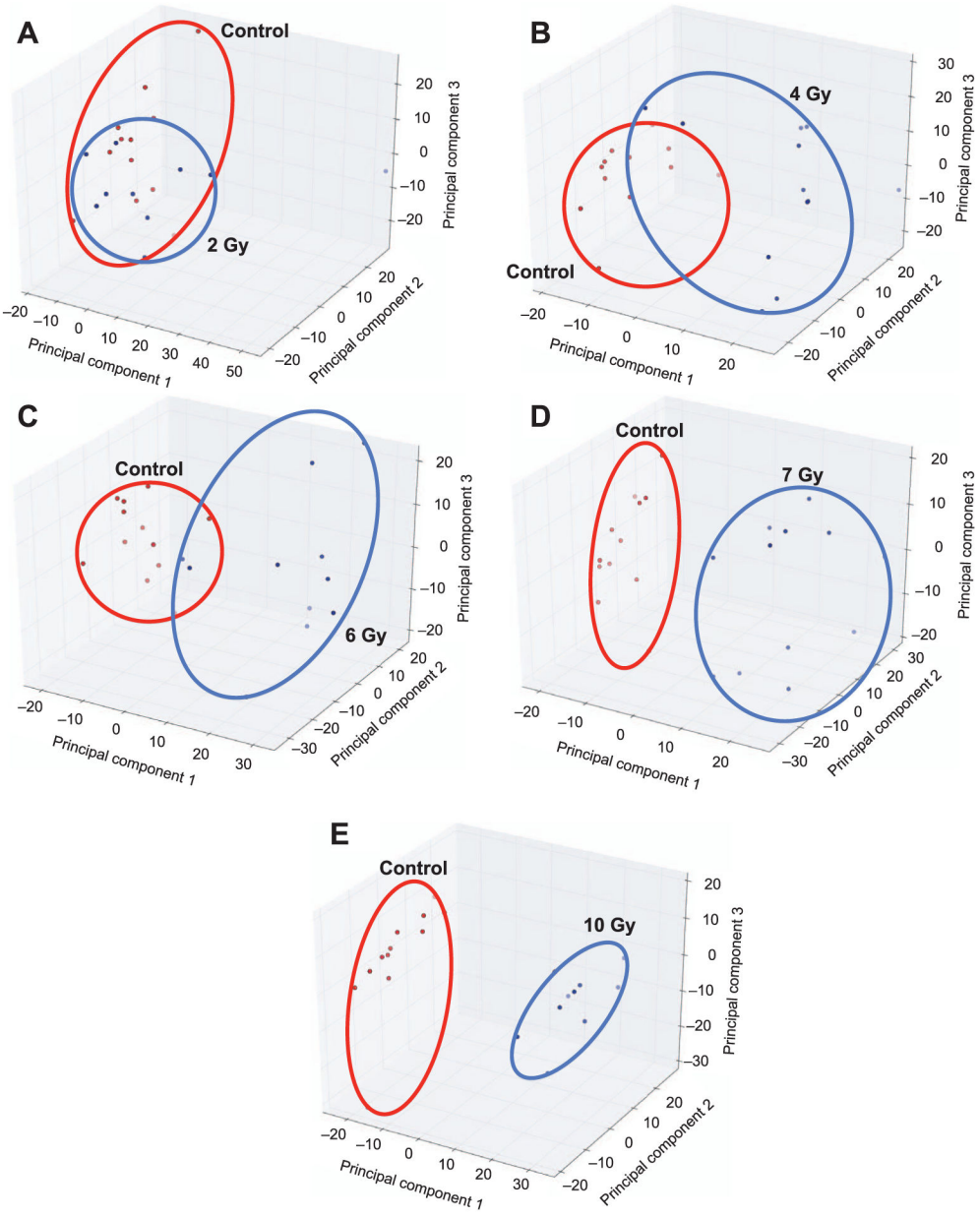

FIG. 3.

Panel A shows unsupervised principal component analysis (PCA) score plots for control NHP urine samples (ESI^+) compared to (panels B–E) NHP urine samples after 2, 4, 6, 7 and 10 Gy gamma irradiation, respectively. Increased separation among the groups occurs with increased doses, suggesting increased metabolic disruption and biomarker excretion. Clear separation between control and irradiated groups is visible at 7 and 10 Gy.

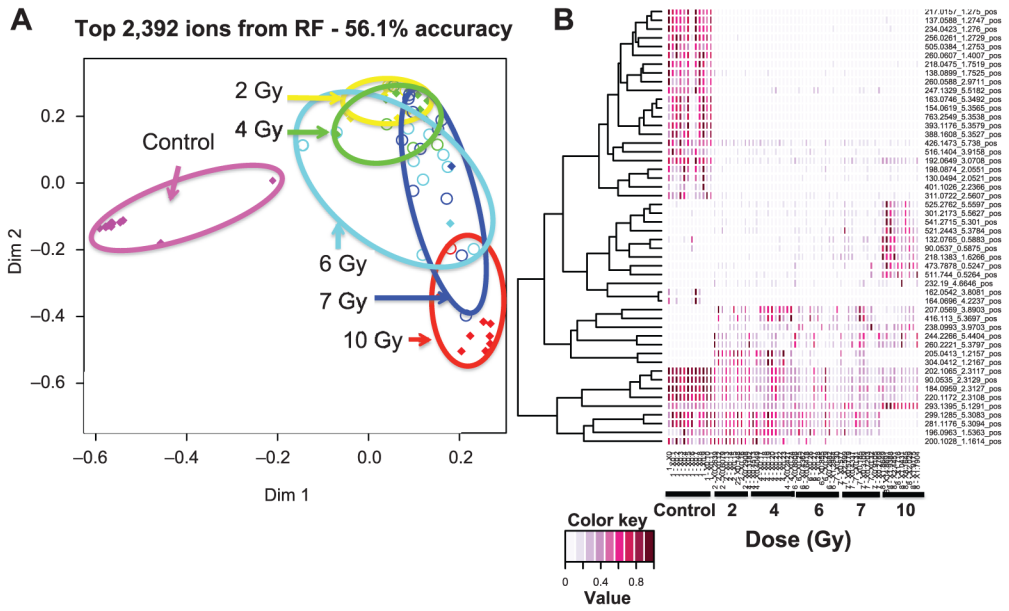

FIG. 4.

Panel A: Multidimensional scaling plot (colored diamonds = correct; colored circles = misclassified) and (panel B) heatmap generated with Random Forests results comparing metabolomic signatures (ESI^+) of urine from NHPs exposed to 2, 4, 6, 7 or 10 Gy γ radiation. Separation between control and irradiated groups is visible, with greater separation at 6, 7 and 10 Gy.

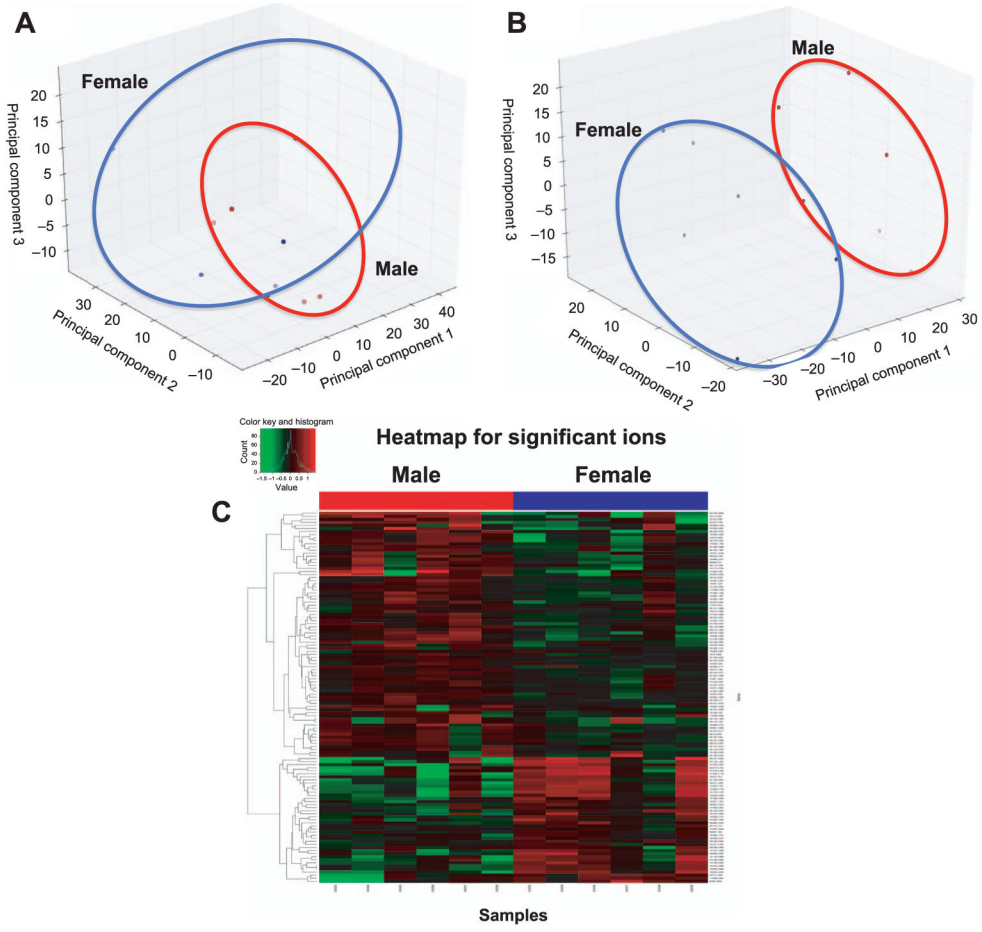

FIG. 5.

Unsupervised principal component analysis (PCA) scores plot comparing male and female control samples (panel A), PCA scores plot (panel B) and heatmap comparing male and female NHP urinary metabolic biosignatures (ESI^+; panel C) after 7 Gy γ irradiation. Slight separation is observed between male and female controls, but separation is more pronounced between irradiated samples. Differences are visible by PCA and heatmap at 7 Gy.

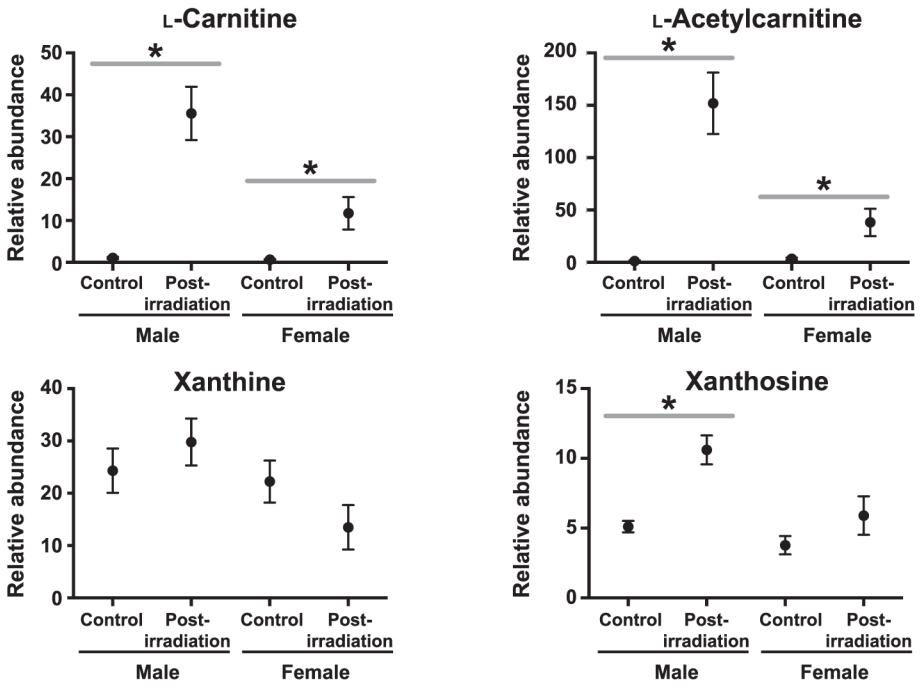

FIG. 6.

Dose response of four validated biomarkers comparing male and female NHP urine after 7 Gy gamma irradiation (* with bar indicates $P < 0.05$ by Welch's *t* test between pre- and postirradiation). Xanthosine, L-carnitine and L-acetylcarnitine are increased in males and females, although males show a higher fold change.

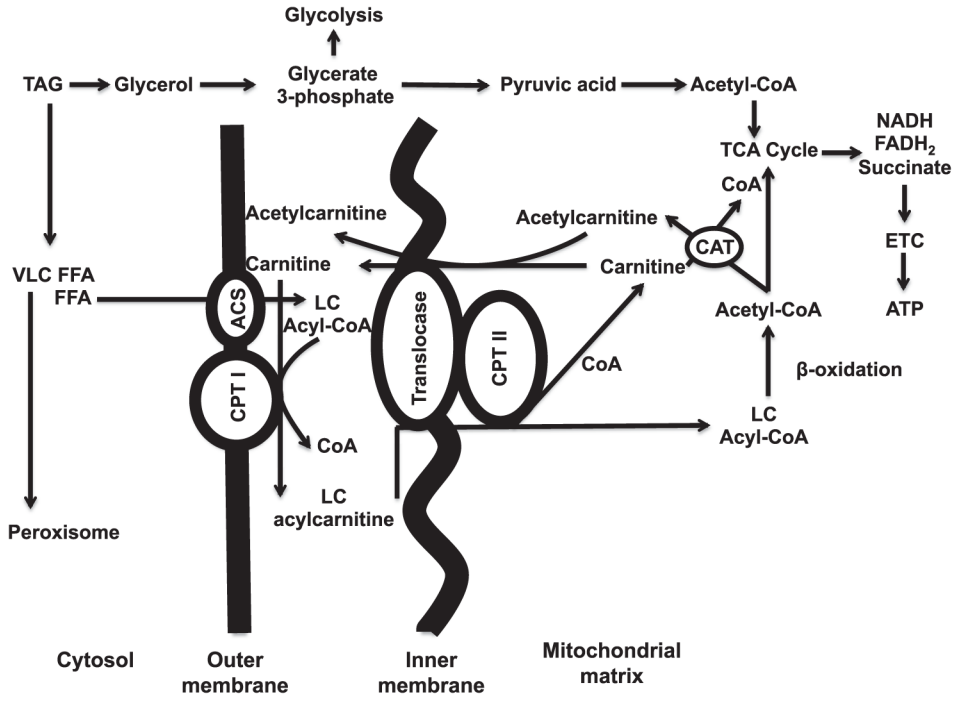

FIG. 7.

Carnitine and acylcarnitine roles in transportation of long-chain fatty acids into the mitochondrial matrix and the β-oxidation pathway. Free fatty acids (FFAs) are transported into the cytosol by fatty acid transport proteins. Very long-chain (VLC) FFAs >22C do not enter the mitochondria and are metabolized by peroxisomes. β oxidation of FFAs results in 2-carbon units (acetyl-CoA) released to enter the TCA cycle. The remaining acyl is further metabolized. Perturbations of the fatty acid β-oxidation pathway may affect energy production. TAG = triacylglyceride; FFA = free fatty acid; VLC = very long chain; LC = long chain; CoA = coenzyme A; CPT = carnitine palmitoyl transferase; CAT = carnitine acyl transferase; GLC = glucose; ETC = electron-transport chain; ACS = acetyl-CoA synthetase.

TABLE 1

Validated Biomarkers of Exposure to Gamma Radiation in Nonhuman Primate Urine

RT min	Experimental m/z	Calculated m/z	Mass error ppm	Formula	ESI mode	Metabolite name
0.52	124.0063	124.0068	8.67	$C_2H_7NO_3S$	Negative	Taurine
0.94	151.0253	151.0256	5.6	$C_5H_4N_4O_2$	Negative	Xanthine
2.70	206.0444	206.0453	1.88	$C_{10}H_8NO_4$	Negative	Xanthurenic acid
1.85	283.0672	283.0679	4.24	$C_{10}H_{12}N_4O_6$	Negative	Xanthosine
0.58	114.0657	114.0667	4.25	$C_4H_7N_3O$	Positive	Creatinine
0.59	132.0765	132.0773	1.93	$C_4H_9N_3O_2$	Positive	Creatine
5.64	363.2181	363.2172	4.14	$C_{21}H_{30}O_5$	Positive	Cortisol
5.65	361.2024	361.2015	4.04	$C_{21}H_{28}O_5$	Positive	Cortisone
0.85	137.0455	137.0463	2.15	$C_5H_4N_4O$	Positive	Hypoxanthine
0.56	162.112	162.113	2.94	$C_7H_{15}NO_3$	Positive	L-Carnitine
0.80	204.1226	204.1236	2.13	$C_9H_{17}NO_4$	Positive	L-Acetylcarnitine
3.00	190.0495	190.0504	1.94	$C_{10}H_7NO_3$	Positive	Kynurenic acid
2.43	232.154	232.1549	1.49	$C_{11}H_{21}NO_4$	Positive	Isobutyryl-L-carnitine/butyrylcarnitine

TABLE 2

Fold Change from Exposure to 10 Gy γ Radiation Compared to Control

Metabolite name	Control (relative intensity)	10 Gy (relative intensity)	*P* value[a]	Fold change
Taurine	0.63 ± 0.08	4.49 ± 0.43	<0.001	7.1
Xanthine[b]	4.24 ± 0.51	6.84 ± 0.72[b]	0.04	1.6
Xanthurenic acid	8.56 ± 1.05	46.97 ± 5.07	<0.001	5.5
Xanthosine	4.44 ± 0.43	13.03 ± 1.19	<0.001	2.9
Creatinine	408.49 ± 28.67	146.23 ± 27.45	<0.001	0.4
Creatine	30.96 ± 16.27	238.69 ± 32.02	<0.001	7.7
Cortisol	2.05 ± 0.46	47.87 ± 16.08	<0.001	23.4
Cortisone	2.32 ± 0.34	8.30 ± 0.58	<0.001	3.8
Hypoxanthine	74.42 ± 6.10	181.84 ± 14.20	0.001	2.4
L-Carnitine	0.84 ± 0.15	55.58 ± 13.20	<0.001	66.2
L-Acetylcarnitine	2.37 ± 0.69	325.69 ± 60.30	<0.001	137.4
Kynurenic acid	82.03 ± 9.48	126.92 ± 11.24	0.003	1.6
Isobutyryl-L-carnitine/butyrylcarnitine	41.64 ± 4.93	205.01 ± 15.55	<0.001	4.9

[a] *P* value from Welch's *t* test.

[b] From 6.0 Gy.

TABLE 3

Urine Biomarkers of Gamma Radiation from Different Species

Metabolite	NHP urine 7 days, 10 Gy	NHP urine 1 day, 8.5 Gy[a]	Human urine 6 h, 1.25 Gy[b]	Mouse urine
Taurine	↑	↑		↑[c]
Xanthine	↑	↑	↑	↑[d]
Xanthurenic acid	↑			
Xanthosine	↑			↑[d]
Creatinine	↓	↑		↑[c]
Creatine	↑	↑		
Cortisol	↑			
Cortisone	↑			
Hypoxanthine	↑	↑	↑	
L-Carnitine	↑			
L-Acetylcarnitine	↑		↓	
Kynurenic acid	↑			
Isobutyryl-L-carnitine/butyrylcarnitine	↑			

[a] Johnson *et al*. (7)

[b] Laiakis *et al*. (8).

[c] 8 Gy, 24 h, Tyburski *et al*. (10).

[d] 3 Gy, 24 h, Tyburski *et al*. (11).